Int. J. Electrochem. Sci., 7 **(2012)** 12764 - 12773

International Journal of
ELECTROCHEMICAL
SCIENCE
www.electrochemsci.org

Efficiency Enhancement with electrodeposition Pt-Ru Bimetallic Nanoparticles and Poly(3,4-ethylenedioxythiophene) Hybrid Film as Counter Electrode in Dye-Sensitized Solar Cells

Tsung-Hsuan Tsai, Cheng-Yu Yang, Shen-Ming Chen[*]

Electroanalysis and Bioelectrochemistry Lab, Department of Chemical Engineering and Biotechnology, National Taipei University of Technology, No.1, Section 3, Chung-Hsiao East Road, Taipei 106, Taiwan (ROC).
[*]E-mail: smchen78@ms15.hinet.net

Received: 13 October 2012 / *Accepted:* 4 November 2012 / *Published:* 1 December 2012

Simple electrodeposition method was employed for the fabrication of platinum-ruthenium bimetallic nanoparticles (PtRu NPs) modified poly(3,4-ethylenedioxythiophene) (PEDOT) coated on the indium tin oxide (ITO) at room temperature. The formation mechanism of PtRu NPs film is monitored by cyclic voltammetry (CV) techniques and atomic force microscopy (AFM). It is found that PtRu NPs/PEDOT/ITO photo cathode increased the reactive interface, which supports charge transfer at the interface and had higher electrocatalytic activity for the I_3^-/I^- redox reaction and a smaller charge transfer resistance than the Pt/ITO photo cathode. With a PtRu NPs/PEDOT/ITO photo cathode as a counter electrode of DSSC, a 16.5% improvement in the cell efficiency is achieved.

Keywords: Dye-sensitized solar cells, Electrodeposition, Electrocatalysis, platinum, ruthenium, PEDOT, N719 dye, Cyclic voltammetry

1. INTRODUCTION

Dye-sensitized solar cell (DSSC) consists of three main components: a dye-covered nano crystalline TiO_2 layer on a transparent conductive glass substrate, an electrolyte contained iodide/triiodide redox couple, and a platinized conductive glass substrate as a counter electrode [1]. Among constituent components in DSSCs, the function of counter electrode is the electron transfer from the external circuit back to the redox electrolyte and catalyzing the reduction of the triiodideion (I_3^-) [2]. Generally, platinum-coated transparent conductive oxide electrode is used as a counter electrode due to its excellent electrocatalytic activity for the I_3^-/I^- redox couple. However, platinum is a noble metal and relatively expensive. Therefore, the cost of the platinum counter electrode represents

more than 40% of the whole DSSC cell cost regardless of its preparation method. Furthermore, the slow dissolution of platinum counter electrode in the corrosive I_3^-/I^- redox electrolyte deteriorates the long term stabilities of DSSCs [3]. Nano ruthenium oxide (RuO_x) is recognized as an important material for a wide range of electrochemical applications including the use of RuO_x as an excellent electrocatalyst for the oxidation of carbon monoxide and methanol oxidation in fuel cells [4, 5], and a promising electrode material used in super capacitors [6, 7].

Conducting polymers have been proposed as counter electrode (CE) in the field of energy production and storage, such as fuel cell [8, 9] and DSSC [10, 11] in order to satisfy the requirements of surface catalytic activity, flexibility. Conducting polymers are a family of outstanding materials for the realization of a quantity of new devices. It is important to realize that, apart from conductivity and flexibility, these polymers are also characterized by other features, such as transport of ions, redox behavior, electrochemical and optoelectronic response. Recently, conducting polymer incorporated metallic or semiconducting nanoparticles provides an exciting system and these materials hold potential application in electronics, sensors and catalysis [12–22]. In this report, we use PEDOT as an electronically conducting polymer. It can be easily electrodeposited onto a surface by the electro oxidation of its monomer [23–25]. A PEDOT film in its oxidized form has been found to have high conductivity and stability at physiological pH [26, 27]. Recently, the PEDOT film always cooperated with other material as the counter electrode used in DSSCs, such as graphene-PEDOT-PSS [28], *f*-MWCNT-PEDOT [29], PEDOT-PSS [30] and PEDOT-PSS-Pt [31]. However, the PEDOT film can be an efficient mediator and enhance the efficiency of DSSC.

In this report, Pt NPs, Ru NPs, and PEDOT were selected to investigate the film formation of biometallic/conducting polymer film modified ITO for the counter electrode of DSSC. The morphology of these films was investigated by and AFM. Electrochemical behaviors were studied by cyclic voltammetry (CV) and x-ray diffraction analysis (XRD). It was observed that PtRu NPs/PEDOT/ITO successfully used as a counter electrode and significantly influenced the performance of DSSCs. The photovoltaic performances of the devices were analyzed.

2. EXPERIMENTAL

2.1 Materials and chemicals

Ruthenium (III) chloride, potassium hexachloroplatinate (IV), 3,4-ethylenedioxythiophene (EDOT), P25 TiO_2 powder, N719 dye, 4-t-butylpyridine (TBP),Triton X-100 solution and PEG 20000 were purchased from Sigma-Aldrich (USA). Dihydrogen hexachloroplatinate (IV) hexahydrate (H_2PtCl_6) was purchased from Alfa Aesar. Indium tin oxide (ITO) (7 $\Omega \cdot cm^{-2}$) was purchased from Merck Display Technologies (MDT) Ltd (Taiwan). Lithium iodide (LiI, analytical grade)was obtained from Wako (Japan). 60 μm thick surlyn films were purchased from Solaronix S.A., Aubonne, (Switzerland). Double distilled deionized water (DDDW) was used to prepare all the solutions.

2.2. Apparatus

All electrochemical experiments were performed using a CHI 410a potentiostat (CH Instruments, USA). The atomic force microscope (AFM) images were recorded using a multimode scanning probe microscope (Being Nano-Instruments CSPM-4000, China).

2.3 Preparation of Photoanode and Photocathode

9 g P25 TiO_2 powder with 0.1 ml Triton X-100, 1g PEG 20000 and 18 ml DDDW were mixed well in a dried agate mortar for one hour. The final mixture was stirred for an additional 2 days to obtain the desired TiO_2 paste. The above obtained TiO_2 paste solution was spin-coated on an ITO glass substrate at 1000 rpm for 10 s and 2000 rpm for 30 s. The formed film was annealed at 450 °C for 1 hour in atmosphere. The PEDOT modified glassy carbon electrodes (PEDOT/GCE) were prepared through the EDOT electro polymerization by cyclic voltammetry [13, 16, 32-33]. An ITO glass was ultrasonically washed with acetone and double-distilled water for 10 min acted as the working electrode in the three-electrode system (Pt wire auxiliary electrode and Ag/AgCl reference electrode) was immersed in the above solution. CV was carried out using a CHI410a electrochemical workstation (CH Instruments, USA) to electrodeposit Pt, Ru and PtRu NPs onto the PEDOT/ITO substrate. The above electrodes were separated by a 60 μm thick surlyn film and sealed together by heating. A thin layer of electrolyte was introduced into the inter electrode space. The electrolyte contains 0.1 M LiI, 0.05 M I_2, and 0.5 M 4-tertbutylpyridine (TBP) in dehydrated acetonitrile.

3. RESULTS AND DISCUSSION

3.1 Surface morphology and XRD analysis of various counter electrodes

The surface morphology of various counter electrodes has been examined using AFM. Here the AFM studies could furnish the comprehensive information about the surface morphology of Pt, Ru and Pt-Ru NPs coated on the PEDOT/ITO and ITO surface. The AFM parameters have been evaluated for 5000 × 5000 nm surface area. From the AFM images, we clearly observed the smallest particles (about 49.5 nm) and a porous structure for bare ITO, Pt, Ru, PtRu, PEDOT, Pt/PEDOT, Ru/PEDOT and PtRu NPs film (Fig. 1A–H). The PtRu NPs and PtRu NPs/PEDOT in the obvious manner were found to 105 nm and 74.8 nm, average height was found as 23.1 nm and 26.9 nm. By AFM roughness analysis, roughness factors obtained are increased by PtRu, Pt, and Ru NPs electrodeposited on PEDOT/ITO as listed in Table 1. The highest roughness factor of PtRu NPs/PEDOT film may be attributed to the PEDOT offers good stability, high conductivity, and acts as a good matrix [13, 14]. The above AFM results clearly illustrate the surface nature of Pt, Ru, and PtRu NPs electrodeposited on the PEDOT/ITO and ITO surface.

The effect of various counter electrodes was investigated using XRD. Fig. 2 showed the XRD patterns of (A) Pt NPs, (B) Ru NPs, (C) PtRu NPs, (D) PEDOT film, (E) Pt NPs/PEDOT, (F) Ru NPs/PEDOT, (G) PtRu NPs/PEDOT.

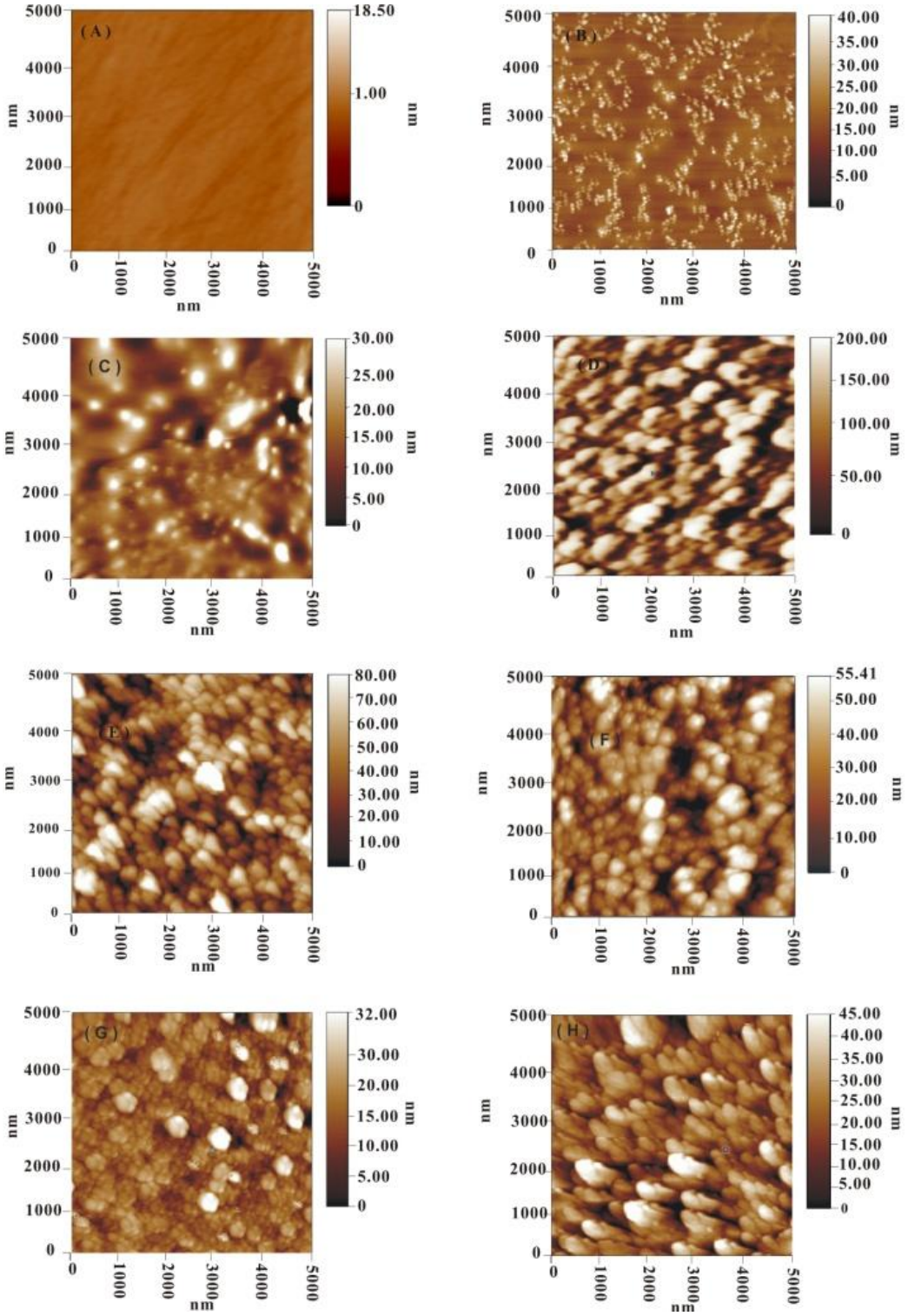

Figure 1. AFM images of (A) ITO, (B) Pt NPs/ITO, (C) Ru NPs/ITO, (D) PtRu NPs/ITO, (E) PEDOT/ITO, (F) Pt NPs/PEDOT/ITO, (G) Ru NPs/PEDOT/ITO, (H) PtRu NPs/PEDOT/ITO.

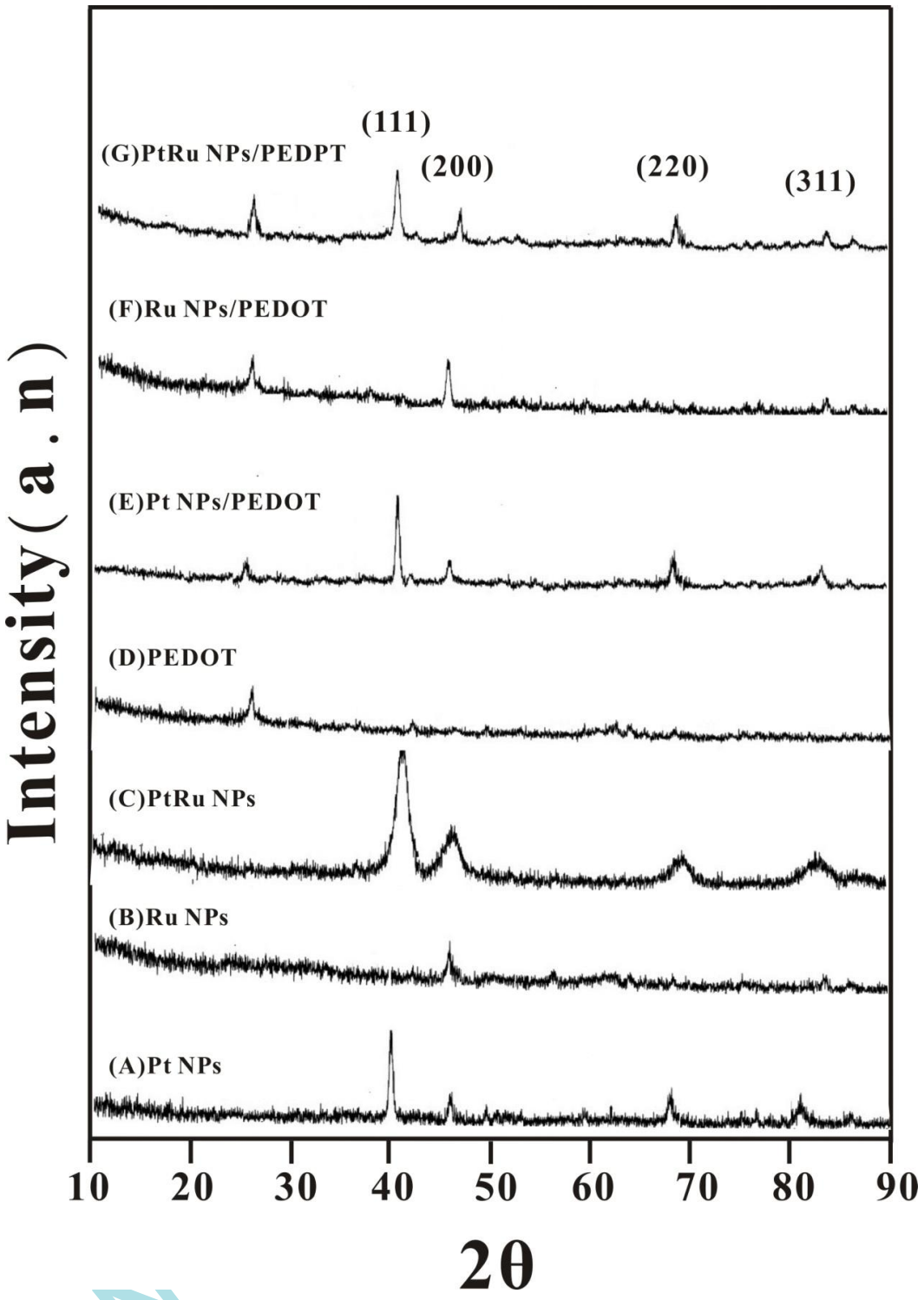

Figure 2. XRD spectra of (A) Pt NPs, (B) Ru NPs, (C) PtRu NPs, (D) PEDOT, (E) Pt NPs/PEDOT, (F) Ru NPs/PEDOT and (G) PtRu NPs/PEDOT/ITO.

For the PtRu NPs/PEDOT, the peaks were found in 39.78°, 45.73°, 68.48° and 83.09° for (111), (200), (220) and (311) [34]. For PEDOT patterns, the peak was found in 21.44°, respectively [35]. All these XRD peaks clearly validate the presence of Pt, Ru, and PtRu NPs on the PEDOT/ITO and ITO surface.

Table 1. Physicochemical properties of DSSCs based on various counter electrodes.

Counter electrode	Parameters Ra (nm)	RMS (nm)	Avg. hight (nm)	Avg. size (nm)
Pt	3.78	5.07	20.15	49.5
Ru	4.55	5.94	17.98	56.3
PtRu	4.11	8.42	23.1	105
PEDOT	2.89	6.95	33.4	47.97
PEDOT-Pt	9.97	12.5	34.3	77.1
PEDOT-Ru	8.64	9.33	30.7	78.5
PEDOT-PtRu	7.31	10.92	26.9	74.8

3.3 Electrocatalytic activity of various CEs

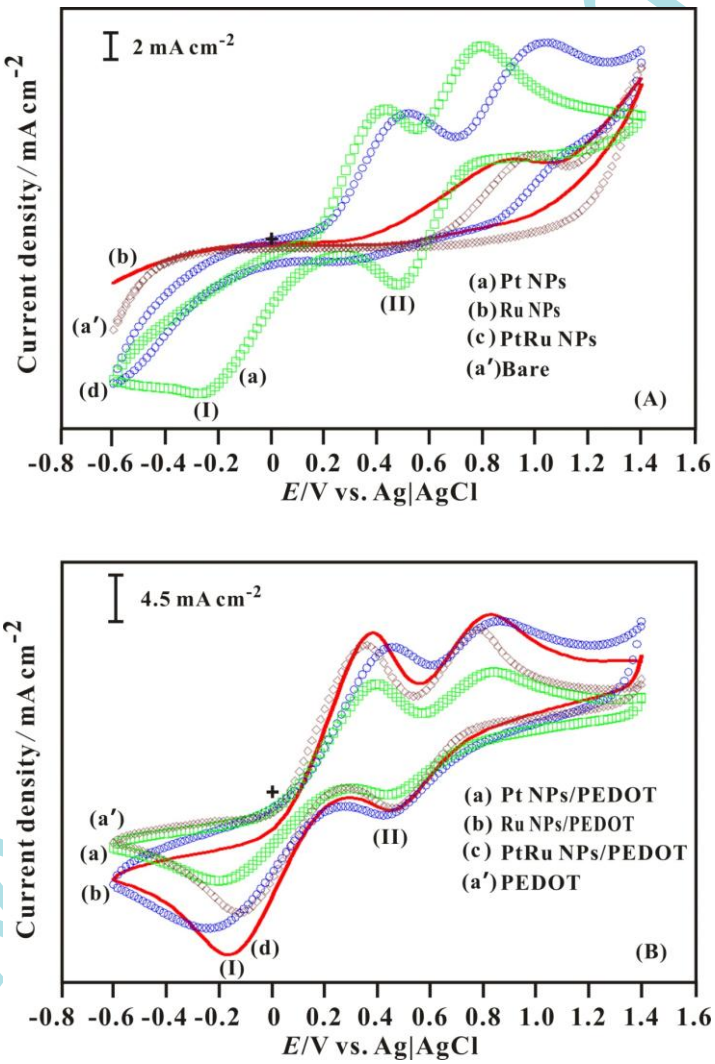

Figure 3. Cyclic voltammograms of (A) (a') ITO, (a) Pt, (b) Ru and (c) PtRu NPs electrodeposited on ITO electrode and (B) (a'), (a) Pt, (b) Ru and (c) PtRu NPs electrodeposited on PEDOT/ITO electrode in an acetonitrile solution with 0.01 M LiI, 0.001 M I_2 and 0.1 M $LiClO_4$, initial E = + 1.6 V, high E = + 1.6 V, low E =−0.4 V, scan rate = 50 mV s^{-1}.

The major function of counter electrode in a DSSC is to serve as a platform for the regeneration of I_3^- to I^- by electrochemical reduction. Accordingly, the electrochemical activities of the prepared thin films with respect to the I^-/I_3^- redox reactions were probed using cyclic voltammetry in this study. Two cathodic peaks of CV were represented the reduction reactions in redox reaction (I) and (II), as shown in Fig. 3 [36].

$$I_3^- + 2e^- \rightarrow 3I^- \quad \text{(I)}$$

$$3I_2 + 2e^- \rightarrow 2I_3^- \quad \text{(II)}$$

Fig. 3A showed the overlaid CVs recorded for (a) PtRu NPs, (b) Pt NPs, (c) Ru NPs on PEDOT/ITO, ITO and bare ITO in an acetonitrile solution with 0.01 M LiI, 0.001 M I_2 and 0.1 M $LiClO_4$. The PtRu NPs/ITO showed two redox peaks and higher current than that the Pt NPs/ITO, Ru NPs/ITO and bare ITO. Compared with various counter electrodes, the bare ITO showed an I_{pc} value close to zero, revealing that it has no catalytic current for the reduction of I_3^-. After electropolymerization PEDOT film on the ITO substrate, the electrochemical activities represented by CV were shown as Fig. 3B (a) PtRu, (b) Pt, (c) Ru NPs, which coated on the PEDOT/ITO and (d) PEDOT/ITO. The absolute I_{pc}*'s* of the CVs showed increases with increasing deposition PtRu NPs. These results suggest that the catalytic current of PtRu NPs/PEDOT layer for I_3^- reduction.

This lack of reactivity is consistent with the poor photovoltaic performance of the DSSC. The reduction peaks of various counter electrodes occurred in the range of -0.6 to +1.4 V (belonging to $I_3^- + 2e^- \rightarrow 3I^-$). The peak potential separations (ΔE_p) of I_3^-/I^- (I_2/I_3^-) for PtRu NPs, Pt NPs and Ru NPs coated on the ITO were 224 (204), 687 (313), ND (ND) (Fig. 3A), and coated on the PEDOT/ITO were 537 (376), 595 (398) and 680 mV (430 mV), respectively (Fig. 3B). The ΔE_p (>>0.059 V/n, n = 2 for I_3^-, n = 2/3 for I_2) indicated that all of the above-mentioned electrode reactions were kinetically controlled and irreversible [37]. The lower ΔE_p and higher catalytic current for the reduction of I_3^- of PtRu NPs/PEDOT film indicated that it had more electrochemically active relative to the others. These findings demonstrate that two inverse effects should be given by the film that increased the active interface and electronic transport resistance in the film.

3.4. Photoelectric performances of DSSCs

Fig. 4 showed the photocurrent-voltage curves of the cells with various counter electrodes, measured at full sunlight of 100 mW cm^{-2} (AM 1.5) conditions and illuminated from the CE side, respectively. The open-circuit voltage (V_{oc}), short-circuit photocurrent density (J_{sc}), fill factor (FF) and efficiency (η%) of the cells are listed in Table 2.

Energy conversion efficiency of DSSCs using PtRu NPs coated on the PEDOT/ITO as counter electrode were measured to be 5.87% and the J_{sc} were also higher than those of the DSSCs with Pt NPs, Ru NPs coated on the PEDOT/ITO and ITO as counter electrode.

Table 2. The photovoltaic parameters of DSSCs based on various counter electrodes.

Counter electrode	J_{sc} (mA cm^{-2})	V_{oc} (V)	FF (%)	□η □(%)
Pt	12.66	0.732	54.36	5.04
Ru	11.48	0.741	49.35	4.20
PtRu	12.84	0.718	53.88	4.97
PEDOT	11.28	0.743	52.21	4.38
PEDOT-Pt	14.83	0.725	51.70	5.56
PEDOT-Ru	11.08	0.758	53.50	4.50
PEDOT-PtRu	16.20	0.693	52.24	5.87

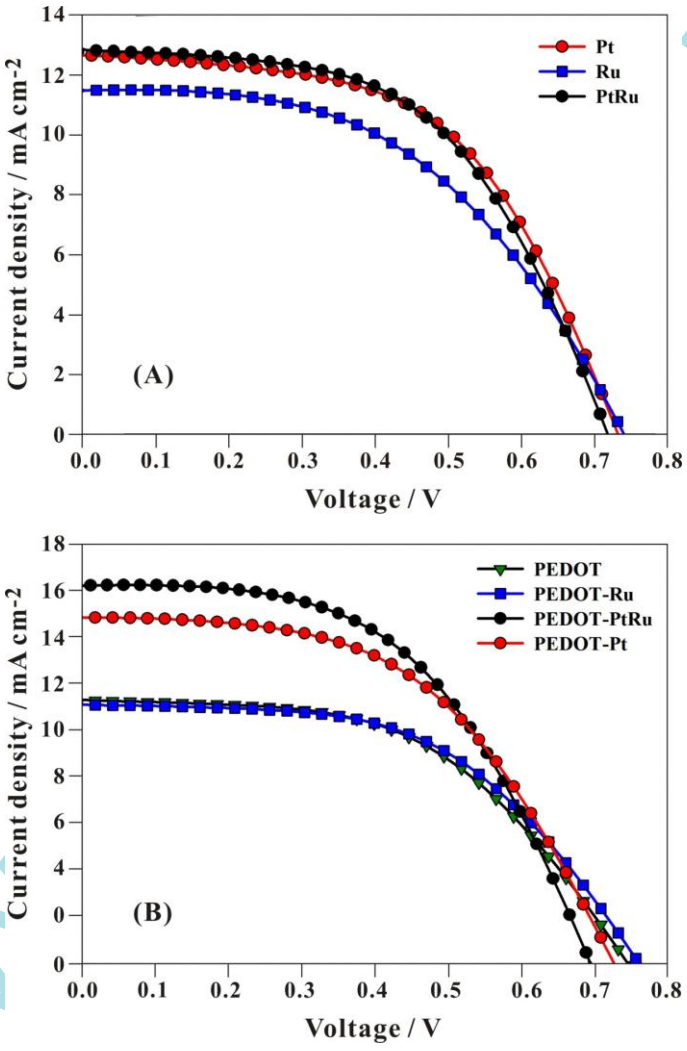

Figure 4. Photocurrent density-voltage curves of DSSCs based on CEs of Pt, Ru and PtRu NPs on (A) ITO and (B) PEDOT/ITO, respectively. The measurements were recorded under 100 mW cm^{-2}, AM 1.5.

Compared to Pt NPs/PEDOT film, the addition of Ru NPs increased the short-circuit photocurrent densities and fill factors of the cells. This is mainly due to that the size of Ru NPs are

small, the particles are in agglomerate form which has resulted in lower power from the cell. Other reason might be that the catalytic efficiency of Pt and Ru NPs may be significantly different [38]. These results indicate that the PtRu NPs/PEDOT/ITO as a counter electrode is sufficient for electrochemical catalyzation and can effectively improve the cell performances.

4. CONCLUSION

In summary, a PtRu NPs/PEDOT/ITO photo cathode has been demonstrated as a means of increasing the efficiency of dye sensitized solar cells. A layer of PEDOT on ITO surface provided a highly porous structure and might easily entrap PtRu NPs. This results in a significant increase in the short-circuit current and the overall power conversion efficiency. It is confirmed that PtRu NPs/PEDOT/ITO photo cathode is an efficient co-catalyst improved the catalyst stability and showed a 16.5% improvement of conversion efficiency than Pt/ITO photo cathode under full sunlight of 100 mW cm^{-2} (AM 1.5) conditions.

ACKNOWLEDGMENT
This work was supported by the National Science Council of Taiwan.

References

1. P. Li, J. Wu, J. Lin, M. Huang, Y. Huang, Q. Li, *Solar Energy*, 83 (2009) 845.
2. T.H. Tsai, S.C. Chiou and S.M. Chen, *Int. J. Electrochem. Sci*., 6 (2011) 3938.
3. C.H. Yoon, R. Vittal, J. Lee, W.S. Chae and K.J. Kim, *Electrochim. Acta*, 53 (2008)2890.
4. T.N. Murakami and M. Grätzel, *Inorganica Chim. Acta*, 361 (2008) 572.
5. Z. Lv, D. Xie, X. Yue, C. Feng, C. Wei, *J. Power Sources* 210 (2012) 26.
6. W. Sugimoto, T. Saida, Y. Takasu, *Electrochem. Commun.* 8 (2006) 411.
7. M. Peckerar, Z. Dilli, M. Dornajafi, N. Goldsman, Y. Ngu, R.B. Proctor, B.J. Krupsaw, D.A. Lowy, *Energy Environ. Sci.* 4 (2011) 1807.
8. T. Kuwahara, H. Ohta, M. Kondo and M. Shimomura, *Bioelectrochemistry*, 74 (2008) 66.
9. J. Wu, Q. Li, L. Fan, Z. Lan, P. Li, J. Lin and S. Ha, *J. Power Sources*, 181 (2008) 172.
10. T.H. Tsai, S.C. Chiou and S.M. Chen, *Int. J. Electrochem. Sci*., 6 (2011) 3333.
11. J.W. Long, K.E. Swider, C.I. Merzbacher, D.R. Rolison, *Langmuir* 15 (1999)780.
12. K.C. Lin, T.H. Tsai and S.M. Chen, *Biosensors and Bioelectronics*, 26 (2010) 608.
13. T.H. Tsai, T.W. Chen and S.M. Chen, *Electroanalysis*, 22 (2010) 1655.
14. T.H. Tsai, K.C. Lin and S.M. Chen, *Int. J. Electrochem. Sci*., 6 (2011) 2672.
15. T.H. Tsai, T.W. Chen, S.M. Chen and K.C. Lin,*Int. J. Electrochem. Sci*., 6 (2011) 2058.
16. T.W. Chen, T.H. Tsai, S.M. Chen and K.C. Lin, *Int. J. Electrochem. Sci*., 6 (2011) 2043.
17. T.H. Tsai, S.H. Wang, S.M. Chen, *Int. J. Electrochem. Sci*., 6 (2011) 1655.
18. T.H. Tsai, Y.C. Huang, S.M. Chen, *Int. J. Electrochem. Sci*., 6 (2011) 3238.
19. T.H. Tsai, S.H. Wang, S.M. Chen, *J. Electroanal. Chem.*, 659 (2011) 69.
20. T.H. Tsai, T.W. Chen, S.M. Chen, *Int. J. Electrochem. Sci*., 6 (2011) 4628.
21. T.H. Tsai, Y.C. Huang, S.M. Chen, M.A. Ali, F.M.A. Alhemaid, *Int. J. Electrochem. Sci*., 6 (2011) 6456.
22. T.H. Tsai, T.W. Chen, S.M. Chen, R. Sarawathi, *Russ. J. Electrochem.*, 48 (2012) 291.

23. C.H. Yoon, R. Vittal, J. Lee, W.S. Chae and K.J. Kim, *Electrochim. Acta*, 53 (2008)2890.
24. T.N. Murakami and M. Grätzel, *InorganicaChim. Acta*, 361 (2008) 572.
25. K.M. Kost, D.E. Bartak, B. Kazee, T. Kuwana,*Anal. Chem.*, 60 (1988) 2379.
26. A.Kitani, T. Akashi, K. Sugimoto, S. Ito, *Synth. Met.*, 121 (2001) 1301.
27. W.H. Kao and T. Kuwana, *J. Am. Chem. Soc.*, 106 (1984) 473.
28. F. Ficicioglu and F. Kadirgan, *J. Electroanal. Chem.*, 430 (1997) 179.
29. A.Drelinkiewicz, M. Hasik and M. Kloc, *Catal. Letters*, 64 (2000) 41.
30. E.T. Kang, Y.P. Ting, K.G. Neoh and K.L. Tan, *Synth. Met.*, 69 (1995) 477.
31. G. Inzelt, M. Pineri, J.W. Schultze and M.A. Vorotyntsev, *Electrochim. Acta*,45 (2000) 2403.
32. V.S. Vasantha, S. M. Chen, *Electrochim. Acta*, 51 (2005) 347.
33. V.S. Vasantha, S. M. Chen, *J. Electroanal. Chem.*, 592 (2006) 77.
34. J. Haglund, F. Fernandez-Guillermet, G. Grimvall, M. Korling, *Phys. Rev. B*, 48 (1993) 11685.
35. C. Arbizzani, M. Biso, E. Manferrari, M. Mastragostino, *J. Power Sources*, 178 (2008) 584.
36. A.I. Popov, D.H. Geske, *J. Am. Chem. Soc.*, 80 (1958) 1340.
37. J. Zhang, T. Hreid, X. Li, W. Guo, L. Wang, X. Shi, H. Su, Z. Yuan, Electrochimica Acta, 55 (2010) 3664.
38. S.P. Somani, P.R. Somani, A. Sato, M. Umeno, *Diamond & Related Materials*, 18 (2009) 497.